

## Characterization of surface charge and zeta potential of colloidal silica prepared by various methods

Gyeong Sook Cho<sup>\*\*\*</sup>, Dong-Hyun Lee<sup>\*</sup>, Hyung Mi Lim<sup>\*</sup>, Seung-Ho Lee<sup>\*</sup>, Chongyoun Kim<sup>\*\*</sup>, and Dae Sung Kim<sup>\*†</sup>

<sup>\*</sup>Eco-Composite Materials Center, Korea Institute of Ceramic Engineering & Technology, Seoul 153-801, Korea

<sup>\*\*</sup>Department of Chemical & Biological Engineering, Korea University, Seoul 136-701, Korea

(Received 12 December 2013 • accepted 16 April 2014)

**Abstract**—Colloidal silica is prepared by hydrolysis of TEOS, direct oxidation of Si powder, condensation of silicic acid, etc. There are differences in surface reactivity of silica particle due to the preparation routes. Therefore, it is useful to evaluate surface properties accurately in order to understand the physiochemical properties of the products. The surface charge density, site density and zeta potential with respect to three types of colloidal silica were estimated and discussed. The surface charge density was different depending on preparation method. It is decreasing in the order of direct oxidation, ion exchange, TEOS hydrolysis. The zeta potential is decreasing in the order of ion exchange, TEOS hydrolysis, direct oxidation. The order in surface charge density is different from that in zeta potential because of the difference in stability depending on the particle size and surface charge density.

Keywords: Colloidal Silica, Surface Property, Zeta Potential, Surface Charge Density, Surface Site Density

### INTRODUCTION

Colloidal silica has been used as a suspension that is stably dispersed in an organic solvent or water of acidity or neutrality and basicity [1]. Silica particle with high hardness, strong bonding characteristics has been used in many applications such as ceramic coatings, finishing of fiber or textile, steel surface treatment, organic-inorganic hybrid coatings, refractory binder, chemical mechanical polishing slurry of silicon or sapphire wafer, and investment casting binder.

Colloidal silica may be prepared by various methods including hydrolysis and condensation of TMOS (Tetramethyl orthosilicate) or TEOS (Tetraethyl orthosilicate) [2], direct oxidation of silicon powder [3,4], peptization [5] or milling of silica gel or powder, ion exchange of sodium silicate [1], electrodialysis of aqueous silicates [6], etc.

Ion exchange method has a process whereby cation exchange resin removes the sodium ion of liquid sodium silicate. The liquid sodium silicate as a starting material is diluted to SiO<sub>2</sub> content of 2-6 w%. When the sodium ion in the diluted sodium silicate is removed by passing through the cation exchange resin, active silicic acid is generated. Silica sol is then prepared through the condensation of silicic acid and growth.

The hydrolysis and condensation method produces the silica sol through hydrolysis and condensation of the alkoxy silane with alkoxy group in the presence of base catalysts. Colloidal silica prepared by this method consists of uniform silica particle and high purity. Direct oxidation method for preparing colloidal silica is started by Si precursor, which is directly oxidized under the base catalysts and

water. This method has advantages of concentrated colloidal silica with uniform particle size through simple preparation process.

Properties of the colloidal silica such as surface charge density, zeta potential, particle size distribution, purity, morphology, concentration of the counter ion, and stability of suspension could be changed in accordance with preparation method or precursors.

When the colloidal silica is mixed with different chemical materials such as dispersant, binder, hardener in order to formulate a painting, stability and compatibility of the silica is also changed due to the surface properties of the particles. Thus, we have to accurately understand the surface properties of the particles according to the preparation method. This understanding may help to choose the silica sol that is the most appropriate for the application being considered. In hydrolysis of TEOS, Blaaderen et al. studied the change of particle morphology (measured by SLS, DLS, TEM) and microstructure measured by NMR-spectroscopy on the component ratio of materials [1]. Dove et al. measured the surface charge density of fumed silica in alkali chloride and alkaline earth chloride solutions, and explained the relationship between surface charge density and the radius of alkali and alkaline earth cations [7]. Also, Labbez et al. investigated the charging (i.e., ionization fraction, surface charge density, etc) and electrokinetic (i.e., zeta potential) behavior of calcium silicate hydrate [8]. There are many research results about each preparation method of colloidal silica and measurement of surface charge properties on the particles. However, until today, there is no study to compare surface properties in accordance with the preparation method of the silica sol.

In this study, the surface properties over three kinds of colloidal silica were investigated using an acid-base titration method and electrophoretic light scattering method. The surface charge density and zeta potentials of colloidal silica were compared. We studied the correlation between the particle charge properties and zeta potentials in accordance with preparation method of colloidal silica.

<sup>†</sup>To whom correspondence should be addressed.

E-mail: dskim@kicet.re.kr

Copyright by The Korean Institute of Chemical Engineers.

**Table 1. Properties of the colloidal silica provided from suppliers**

Sample name	SiO <sub>2</sub> concentration (wt%)	pH	ICP analysis*		BET		Product code	Supplier
			Na <sub>2</sub> O (wt%)	C (wt%)	S <sub>BET</sub> (m <sup>2</sup> /g)	D <sub>BET</sub> ** (nm)		
Si 100	40	10.5	0.364	0.027	33.9	81	YGS-40XL	Young il Chemical
SS 100	50	8.8	0.355	0.033	26.7	102	ST-ZL (SNOWTEX)	Nissan Chemical
TE 100	35	6.8	<0.01	0.105	26.9	101	SG-SO100	Suk gyung AT

\*ICP analysis was measured in stock silica sol

\*\*D<sub>BET</sub> was calculated from D<sub>BET</sub>=6000/(ρ<sub>p</sub> SSA), ρ<sub>p</sub>=2.2 g/cm<sup>3</sup>

## MATERIALS AND EXPERIMENTAL METHODS

Three types of ~100 nm colloidal silica, which were prepared by direct oxidation of Si powder, ion exchange of sodium silicate and hydrolysis of TEOS, were provided from Youngil Chemical, Nissan Chemical, Sukgyung AT, respectively. As shown in Table 1, properties of commercial silica sol were summarized by counter ion content, pH, BET, and D<sub>BET</sub> values measured by ICP, pH meter and BET analyzer, respectively. The pH and ionic strength of three types of 20 wt% diluted suspension were adjusted by using NaOH and NaCl in order to maintain the same as pH and ionic strength of each sample. Ion conductivity and pH of the adjusted suspension was 10 mS/cm and pH 10, respectively.

Also, for carrying out acid-base titration experiments, the diluted suspensions of 20 wt% silica were once more diluted using a 0.1 M NaCl solution to a silica concentration of 50 g/L. Each sample was agitated by a magnetic stirrer and purged with pure N<sub>2</sub> (99.999%) for 12 hr, to avoid contamination by atmospheric CO<sub>2</sub>. To avoid the troublesome region, the titration was carried out from pH 3 to 10. Above pH 10, the solubility increases markedly and below pH 3, colloidal silica is coagulated. So, the diluted suspension was first acidified using the 0.1 M HCl to a pH 3 and then back-titrated with the 0.05 M NaOH at the rate of 0.5 ml/min, until the pH 10. Also, acidimetric supernatant, prepared by centrifuging the acid-titrated suspension at 18,000 rpm for 5 hr and separated by filtering the supernatant using a 0.1 μm membrane filter, was utilized as the blank solution.

The samples for zeta potential measurement were diluted to 1-10 wt% (volume fraction of 0.005-0.048). All concentrations were made by diluting the 20 wt% suspension with 10<sup>-3</sup> M NaCl solution. Volume fraction was calculated by Eq. (1) and ρ<sub>sus</sub> was calculated by Eq. (2) [9]:

$$\Phi = \omega \rho_{\text{sus}} / \rho_p \quad (1)$$

$$\rho_{\text{sus}} = \rho_e \frac{1}{1 + \omega \left( \frac{\rho_e}{\rho_p} - 1 \right)} \quad (2)$$

where, Φ is the volume fraction, ω is the concentration of silica, ρ<sub>sus</sub> is the density of diluted suspension, ρ<sub>p</sub> is the density of silica (2.2 g/cm<sup>3</sup>), ρ<sub>e</sub> is the density of water (1.0 g/cm<sup>3</sup>). These diluted samples were stirred for 1 hr and sonicated for 1 min to remove air bubbles. And then, zeta potential and ion conductivity of the samples were measured. The zeta potential of the particles was analyzed by using an ELS-Z (Otsuka Electronics, Japan). To improve reliability of measurements, four measurements of the mobility were aver-

aged. The mobility of particles was measured between two stationary layers where electro osmotic flow was zero in an electric field of 70 V/m<sup>2</sup>. The surface charge density and site density of the samples were analyzed using a 719-S Titrino (Metrohm, USA) to evaluate the surface charge properties of particles. The titration curve was converted to gran plot, and surface properties of the particles were evaluated by calculating the σH (surface charge density), Hs (surface site concentration), Ds (surface site density). Also, the morphology of silica particles was observed through TEM (transmission electron microscopy, JEM-2000, JEOL). The sample was diluted to 5 wt% for TEM measurement. The samples were dropped on the TEM grid, the grid which was dried in an oven at 60 °C for at least 6 hrs. Then, samples were observed at 200,000 magnification.

## RESULTS AND DISCUSSION

### 1. Comparison of Surface Charge between Different Colloidal Silicas

Acid-base titration was conducted to study the surface proton reactions of colloidal silica in Table 1. Three different colloidal silica of ~100 nm are shown in Fig. 1 as TEM images. By data of the sigmoid curves obtained from titration of the samples and blank solutions (supernatant solution without silica particles), the blank solution (i.e., acidimetric supernatant) showed a certain pH buffering capacity. This implies that some reactions consuming the added OH<sup>-</sup> occur in the solution phase, such as the hydrolysis of silicic acid, of which arise from disassociation of silica particle substrate during the acid attack. To subtract the influence of solid dissolution on the estimation of proton or hydroxide ion consumption, it is needed to regard titration blanks. To do Gran plots, the values of the G on acidic side or alkaline side are given by function (3) and (4):

$$\text{On the acidic side : } G_a = (V_0 + V_a + V_b) \cdot 10^{-pH} \cdot 100 \quad (3)$$

$$\text{On the alkaline side : } G_b = (V_0 + V_a + V_b) \cdot 10^{-(13.8-pH)} \cdot 100 \quad (4)$$

where, V<sub>0</sub> represents the initial volume of the suspension, V<sub>a</sub> and V<sub>b</sub> are the total volume of acid solution and OH<sup>-</sup> added at the different titration points, respectively.

Thus, the Gran plot has an acid region and alkali region, and will have a linear region before equivalence, with acidic slope and a linear region after equivalence, with alkaline slope. Fig. 2(a)-(c) are presented as Gran plot regarding Si 100, SS 85, TE 100 samples and blank solutions. The x-intercept, V<sub>ab1</sub> or V<sub>ab2</sub>, corresponds to the equivalence volume obtained by linear regression analysis of the slopes in the Gran plots. Apparent volumes of consuming OH<sup>-</sup> in surface reactions except simple acid-base neutralization of surplus protons,

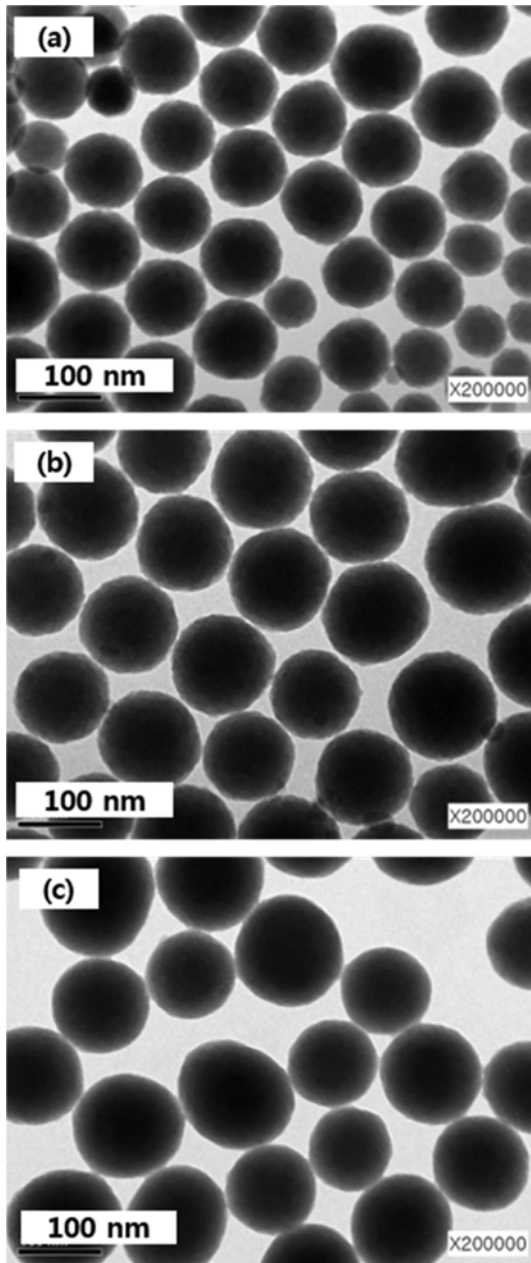


Fig. 1. TEM images of (a) Si 100 by direct oxidation, (b) SS 100 by ion exchange and (c) TE 100 by hydrolysis.

namely  $\nabla V = (V_{ab2} - V_{ab1}) - (V'_{eb2} - V'_{eb1})$  are 4.483, 2.160, 1.859 ml in Si 100, SS 85 and TE 100 samples, respectively. Also, the point of zero charge (pzc) as electrical describes the condition when the electrical charge density on a surface is zero, e.g., it is the pH value at which a particle in an electrolyte exhibits zero net electrical charge on the surface. pH at  $V_{eb1}$  that is starting point of reaction on the particle surface is referred to as PZC (point of zero charge), and PZC of Si 100, SS 85, TE 100 is pH 4.34, 4.62, 4.80, respectively. These PZC values are higher than intrinsic IEP (iso electric point) of the silica. PZC of silica sol is commonly reported to be pH 2-3 in many references, but some references have higher values than it, Schwarz et al. [10] reported a value of 4.1 and Dove et al. [7] the value of ~3, where surface charge density is below 0.01 C/m<sup>2</sup> and

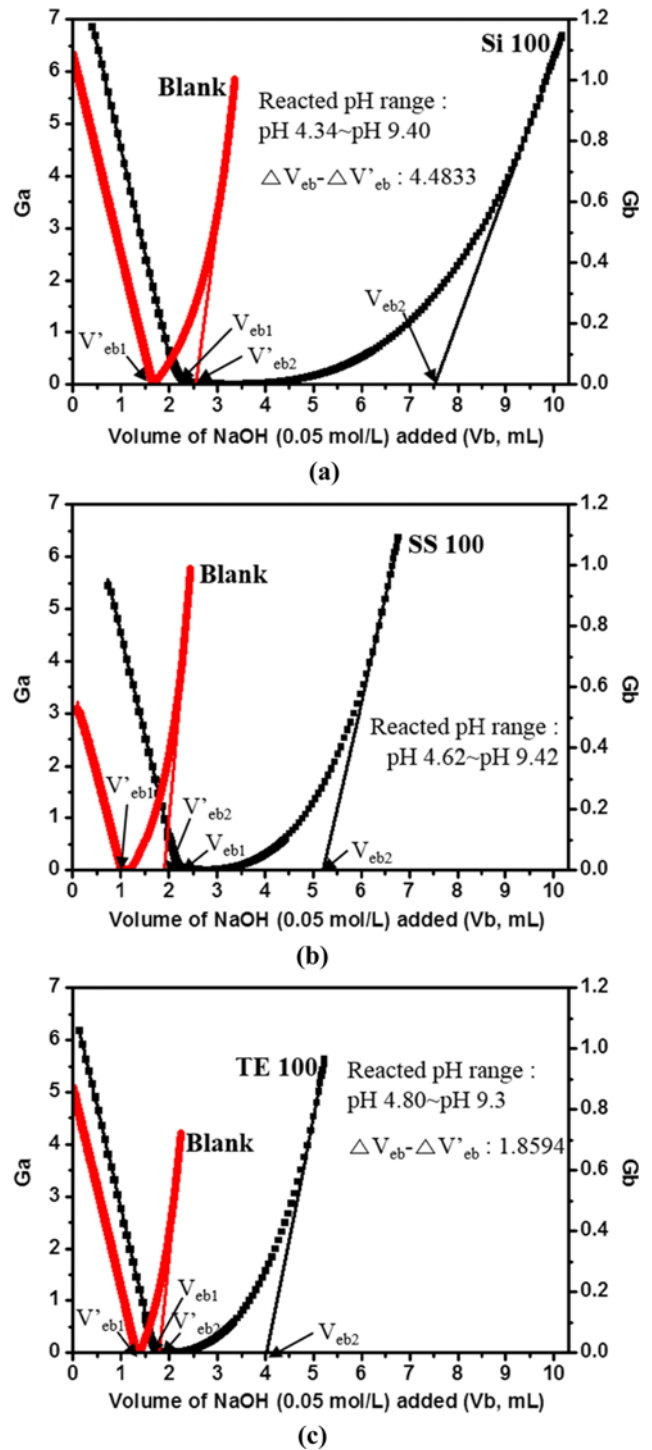


Fig. 2. Gran plot of (a) Si 100 by direct oxidation, (b) SS 100 by ion exchange and (c) TE 100 by hydrolysis.

the graph of it is plateau at vicinity of the PZC not to be clear. But PZCs of each sample are pH 4.34, 4.62 or 4.80, respectively, and the values were somewhat higher than the above expected values.

We have calculated the surface charge density taking BET value under the equation shown below [11].

$$\sigma_H = \left( \frac{F}{C_p S_{BET}} \right) (TOH - [H^+] - [OH^-]) \tag{5}$$

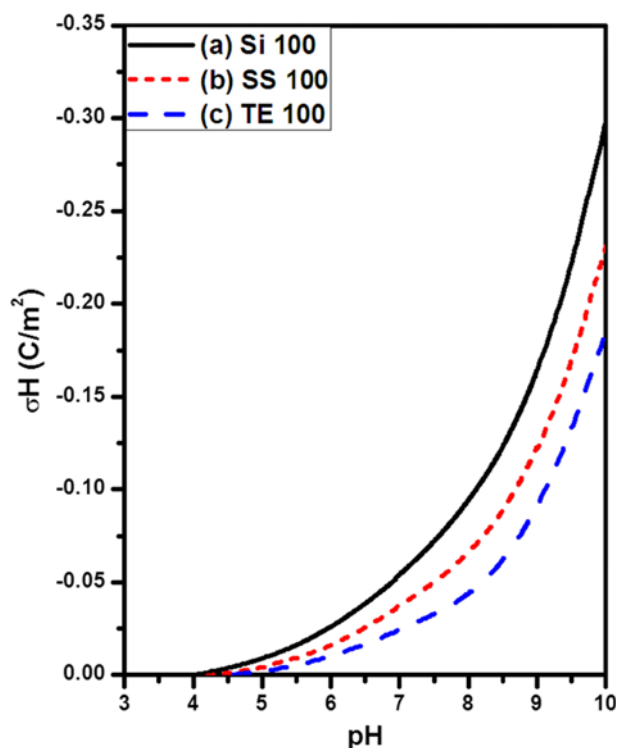


Fig. 3. Surface charge density of (a) Si 100 by direct oxidation, (b) SS 100 by ion exchange and (c) TE 100 by hydrolysis.

where,  $F$  is the Faraday constant (96,485 Coulomb/mol),  $C_p$  is silica concentration,  $S_{BET}$  is specific surface area of silica.

Calculated surface charge density graph according to Eq. (5) is depicted in Fig. 3. Si 100 has more negative surface charge per unit area than SS 100 and TE 100. This effect can be explained by greater replacement of surface  $H^+$  by Na at 0.1 M of NaCl. This result is ascertained through calculation of  $H_s$  (surface site concentration) and  $D_s$  (surface site density) using Eqs. (6) and (7). To calculate the values of sites of samples, it should be considered to subtract the value of blank solution from the value of sample. In this study,  $H_s$  was derived from two equivalent points in the Gran plots of the back-titration, as expressed by Eq. (6).

$$H_s = \frac{(V_{eb2} - V_{eb1})_{sample} \cdot C_b (V_{eb2} - V_{eb1})_{blank} \cdot C_b}{V_0} \quad (\text{mol L}^{-1}) \quad (6)$$

where,  $C_b$  is the concentration of NaOH.

And the equation for  $D_s$  is shown below:

$$D_s = \frac{(H_s \cdot N_A)}{S_{BET} \cdot C_p \cdot 10^{18}} \quad (\text{sites nm}^{-2}) \quad (7)$$

where,  $N_A$  is Avogadro's number ( $6.022 \cdot 10^{23}$  sites  $\text{mol}^{-1}$ ),  $S_{BET}$  is specific surface area of silica and  $C_p$  is the silica concentration.

The  $H_s$  and  $D_s$  on the each silica sol are presented in Table 2 and

Table 2. Surface site concentration ( $H_s$ ) and Surface site density ( $D_s$ ) of colloidal silica prepared by different method

	Si 100	SS 100	TE 100
$H_s$ (mmol/L)	3.7361	1.8000	1.5495
$D_s$ (sites/nm <sup>2</sup> )	1.3257	0.8121	0.6933

they are in the order of Si 100 > SS 100 > TE 100. From among these colloidal silicas, TE 100 having a few sites was prepared by hydrolysis and condensation of TEOS. Then, ethanol was produced from TEOS with ethoxy group through hydrolysis. The hydrolyzed TEOS is converted into a mineral-like solid via the formation of Si-O-Si linkages. Thus, it is estimated that the number of TE 100 sites is fewer than the number of Si 100 and SS 100 because  $OH^-$  ion of NaOH reacted incompletely with surface site due to hydrogen-bond between produced alcohol and silanol group of particle surface. Table 1 shows that the existence of ethanol or ethoxy group on the silica particles could be confirmed from C contents of ICP results on the each stock silica suspension. Also, when the particles grow, the number of available silanol groups slowly decreases [1]. As mentioned above, in Fig. 3, the surface charge density of Si 100, SS 100 and TE 100 follows the same trends as expected. The surface charge of the particles increases with the number of surface site and the Si 100 is considered to have the highest surface charge because of having large number of sites while TE 100 have a relatively lower surface charge due to smaller number of sites than other samples. Resultantly, the concentration of the surface site related to the surface charge density is very dependent on the particle production methods.

## 2. Effect Of Different Colloidal Silica and Volume Fraction on Zeta Potential

For silica sols prepared according to various methods, the zeta potentials on volume fraction of sol were measured and the results are shown in Fig. 4. As shown, the zeta potential of SS 100 is the highest absolute value over total range of the volume fraction, but that of Si 100 is the lowest. In addition, when the volume fraction increases from 0.005 to 0.023, absolute value zeta potential also rises and then shows a decrease for volume fraction higher than 0.023. Originally, the zeta potential depends on the electrostatic repulsion and Debye length. Of these, Debye length is inversely proportional to the square root of ion concentration and charge valence of an ion [12]. In this experiment, the silica sol for ion conductivity measurement was diluted with 0.1 M NaCl, thus showing the standard deviation of maximum 14% in ion conductivity within the same volume fraction as depicted in the Table 3. Thus, it was considered that almost same amount of electrolyte will not affect values of zeta

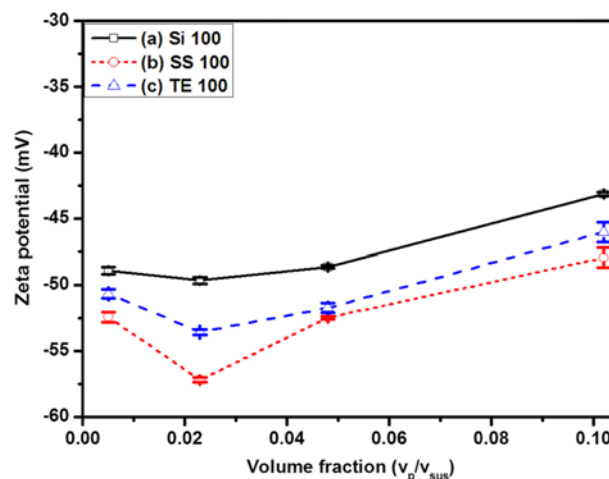
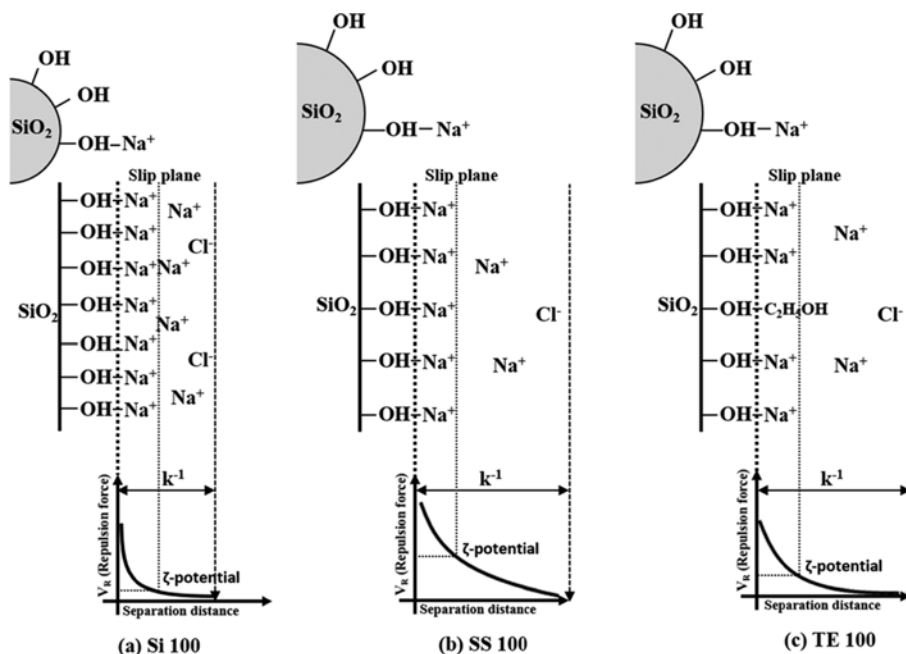


Fig. 4. Zeta potential of (a) Si 100 by direct oxidation, (b) SS 100 by ion exchange and (c) TE 100 by hydrolysis at pH 10.

**Table 3. Ion conductivity of colloidal silica obtained during the zeta potential measurement at different volume fraction**

Sample name	Volume fraction	0.005	0.023	0.048	0.102
Ion conductivity (mS/cm <sup>2</sup> )	Si 100	0.175	0.791	1.478	2.890
	SS 100	0.184	0.817	1.659	2.632
	TE 100	0.180	0.810	1.622	2.674

**Fig. 5. Schematic diagram illustrating relationship between surface charge density and zeta potential (or electric double layer) of (a) Si 100 by direct oxidation, (b) SS 100 by ion exchange and (c) TE 100 by hydrolysis.**

potential and therefore the electrostatic repulsion force will be major contribution. The high electrostatic repulsive force that originated from high surface charge means that the zeta potential is high. Thus, the order of the zeta potential was expected to Si 100 sample > SS 100 sample > TE 100 sample as the same order of magnitude of the surface charge density. However, the order of the zeta potential was different from expectation. Even though the Si 100 sample has the highest surface charge density, it has the lowest zeta potential.

The particle size of Si 100, SS 100, and TE 100 sample measured by BET is 81 nm, 102 nm, and 101 nm, respectively, as shown in Table 1. We pointed out in a previous study [13] that the zeta potential decreases as particle size decreases due to the reduction in electrostatic repulsion force between the particles, which means low total energy barrier on a particle. Therefore, the existence of agglomerated particles in dispersed solution causes a decrease in mobility of the particles and thereby a decrease in zeta potential. According to the previous study, the mobility of 12 nm silica (Lu 12) and 100 nm silica (SC 100) prepared by ion exchange of sodium silicate is dependent on particle size. However, the mobility of 50 nm silica (YC 60) prepared by direct oxidation of silicon powder is lower than Lu12, even though the particle size of YC60 estimated by the BET method is four-times larger than that of Lu12. Therefore, we postulated that the high surface charge density may cause high Na counter ion adsorption on the surface of silica, which results to lower

the mobility and lower zeta potential. The excessive absorption of Na ions on the surface of silica particles may cause reduction in the thickness of the electric double layer and eventually decreases in the zeta potential [14]. Likewise, the zeta potential of Si 100 showing the minimum value among three is believed to be affected by the size of the particles and surface property which was described by surface charge density as mentioned above. Fig. 5 shows a schematic diagram illustrating surface charge density and zeta potential (or electrical double layer) of silica particle prepared by different methods. As shown in Fig. 5, the surface charge density related to surface site of a particle is in the order of (a) Si 100 > (b) SS 100 > (c) TE 100, while the zeta potential value related to Debye length of a particle is in the order of (b) SS 100 > (c) TE 100 > (a) Si 100. Even though SS 100 has higher Na counter ion concentration than TE 100, a higher zeta potential of SS 100 than that of TE 100 is observed. It may be explained by relatively high residual C content which must be originating from the starting material of TEOS as shown in Table 1.

## CONCLUSION

By using a potentiometric titration method, we compared the surface properties of the silica sols prepared by various methods including direct oxidation of silicon powder, ion exchange of sodium silicate,

hydrolysis and condensation of TEOS. As a result, surface charge density was different depending on preparation method. It is decreasing in the order of direct oxidation, ion exchange, TEOS hydrolysis. The value of surface site concentration (Hs) and surface site density (Ds) of samples follows the same trend while the zeta potential is decreasing in the order of ion exchange, TEOS hydrolysis, direct oxidation. The order in surface charge density is different from that in zeta potential because of difference of stability depending on the particle size and surface charge density and concentration of Na ions absorbed on surface of particle.

#### ACKNOWLEDGEMENT

This work supported by KICET and Korea University.

#### REFERENCES

1. H. E. Bergna and W. O. Roberts, *Colloidal silica: Fundamentals and applications*, CRC Press, Boca Raton, FL (1994).
2. S. L. Chen, P. Dong, G. H. Yang and J. J. Yang, *Ind. Eng. Chem. Res.*, **35**, 4487 (1996).
3. H. M. Lim, H. C. Shin, S. H. Huh and S. H. Lee, *Solid State Phenomena*, **124**, 667 (2007).
4. J. Y. Kim, Korea Patent, 10-2000-0045376 (2000).
5. Y. Lee, Y. R. Yoon and H. Rhee, *Colloids Surf.*, **173**, 109 (2000).
6. R. K. Iler, US Patent, 881,371 (1972).
7. P. M. Dove and C. M. Craven, *Geochimica et Cosmochimica Acta*, **69**, 4963 (2005).
8. C. Labbez, B. Jönsson, I. Pochard, A. Nonat, and B. Cabane, *J. Phys. Chem. B*, **110**, 9219 (2006).
9. Z. Adamczyk, B. Jachimska and M. Kolasnińska, *J. Colloid Interface Sci.*, **273**, 668 (2004).
10. J. A. Schwarz, C. T. Driscoll and A. K. Bhanot, *J. Colloid Interface Sci.*, **97**, 55 (1984).
11. Z. Chu, W. Liu, H. Tang, T. Qian, S. Li, Z. Li and G. Wu, *J. Colloid Interface Sci.*, **252**, 426 (2002).
12. U. Paik, J. Y. Kim and V. A. Hackley, *Mater. Chem. Phys.*, **91**, 205 (2005).
13. G. S. Cho, D.-H. Lee, D. S. Kim, H. M. Lim, C. Y. Kim and S.-H. Lee, *Korean Chem. Eng. Res.*, **51**, 622 (2013).
14. J. S. Ko, Y. J. Kwark, M. S. Khil, Y. D. Kim, J. H. Kim, H. D. Ghim, D. I. Yoo, Y. S. Shin, T. H. Oh, W. J. Lee and H. G. Jeong, Chonnam National University Press, Korea (2008).